Exploration of magnetic field generation of H_3^{2+} by direct ionization and coherent resonant excitation

Zhi-Jie Yang(杨志杰), Qing-Yun Xu(徐清芸), Yong-Lin He(何永林), Xue-Shen Liu(刘学深), and Jing Guo(郭静)
Citation: Chin. Phys. B, 2021, 30 (**12**): 123203. DOI: 10.1088/1674-1056/ac0346
Journal homepage: http://cpb.iphy.ac.cn; http://iopscience.iop.org/cpb

What follows is a list of articles you may be interested in

Probing time delay of strong-field resonant above-threshold ionization

Shengliang Xu(徐胜亮), Qingbin Zhang(张庆斌), Cheng Ran(冉成), Xiang Huang(黄湘), Wei Cao(曹伟), and Peixiang Lu(陆培祥)
Chin. Phys. B, 2021, 30 (**1**): 013202. DOI: 10.1088/1674-1056/abc7a5

Laser-assisted XUV double ionization of helium atoms: Intensity dependence of joint angular distributions

Fengzheng Zhu(朱风筝), Genliang Li(黎根亮), Aihua Liu(刘爱华)
Chin. Phys. B, 2020, 29 (**7**): 073202. DOI: 10.1088/1674-1056/ab90ef

Coherent 420 nm laser beam generated by four-wave mixing in Rb vapor with a single continuous-wave laser

Hao Liu(刘浩), Jin-Peng Yuan(元晋鹏), Li-Rong Wang(汪丽蓉), Lian-Tuan Xiao(肖连团), Suo-Tang Jia(贾锁堂)
Chin. Phys. B, 2020, 29 (**4**): 043203. DOI: 10.1088/1674-1056/ab75d9

Ellipticity-dependent ionization yield for noble atoms

Hristina Delibašić, Violeta Petrović
Chin. Phys. B, 2019, 28 (**8**): 083201. DOI: 10.1088/1674-1056/28/8/083201

Quantal studies of sodium 3p←3s photoabsorption spectra perturbed by ground lithium atoms

N Lamoudi, F Talbi, M T Bouazza, M Bouledroua, K Alioua
Chin. Phys. B, 2019, 28 (**6**): 063202. DOI: 10.1088/1674-1056/28/6/063202

Exploration of magnetic field generation of H_3^{2+} by direct ionization and coherent resonant excitation*

Zhi-Jie Yang(杨志杰), Qing-Yun Xu(徐清芸), Yong-Lin He(何永林), Xue-Shen Liu(刘学深), and Jing Guo(郭静)†

Institute of Atomic and Molecular Physics, Jilin University, Changchun 130012, *China*

(Received 8 March 2021; revised manuscript received 11 May 2021; accepted manuscript online 20 May 2021)

Coherent electronic dynamics are of great significance in photo-induced processes and molecular magnetism. We theoretically investigate electronic dynamics of triatomic molecule H_3^{2+} by circularly polarized pulses, including electron density distributions, induced electronic currents, and ultrafast magnetic field generation. By comparing the results of the coherent resonant excitation and direct ionization, we found that for the coherent resonant excitation, the electron is localized and the coherent electron wave packet moves periodically between three protons, which can be attributed to the coherent superposition of the ground A' state and excited E^+ state. Whereas, for the direct single-photon ionization, the induced electronic currents mainly come from the free electron in the continuum state. It is found that there are differences in the intensity, phase, and frequency of the induced current and the generated magnetic field. The scheme allows one to control the induced electronic current and the ultrafast magnetic field generation.

Keywords: ultrafast magnetic field generation, electronic ring current, coherent resonant excitation, direct single-photon ionization

PACS: 32.80.–t, 32.90.+a, 42.25.Kb, 42.65.Re **DOI:** 10.1088/1674-1056/ac0346

1. Introduction

To explore quantum dynamics by using ultrafast laser pulses on its intrinsic time scale is an area of current interest. The rapid development of the techniques of attosecond pulse generation, has become an important tool for investigating electronic dynamics on its natural attosecond time scale and sub-nanometer dimension. And it also promotes the development of some optical imaging technologies, such as Coulomb explosion,[1,2] laser-induced electron diffraction.[3–6] Now the shortest 43-as pulses can be used for new ultrafast optical imaging.[7] Ultrafast negative charge migration illustrates the electron dynamics on attosecond time scale, which is a fundamental quantum process in many biological and chemical reactions.[8,9] This process can be used for selective laser excitation in molecules.[10,11] Besides, coherent superposition of electronic states leads to an electronic ring current inside the molecule,[12,13] which is of latent applied value on molecular magnetism and can be used as a new source of ultrafast magnetic field. Recent experiments demonstrate that people can precisely manipulate the spatial distribution of currents in the semiconductor and subsequently control the ultrafast magnetic field generation.[14] Exploring the time-dependent ultrafast magnetic field that depends on the electronic coherence may provide a direct way to access and control the electronic quantum coherence dynamics in photophysical and photochemical reactions in real time. Optically induced magnetic fields are also used as tools for investigating new phenomena in molecular and material sciences.[15–19] Now a lot of researches have shown that the ultrafast magnetic fields can be efficiently produced in molecules from electronic ring currents.[20,21] Results show that the laser-induced magnetic fields generated by electronic currents are static and can be much larger than those obtained by traditional methods about static field.[22] Therefore, it is of great significance to the development of molecular magnetism. However, most of researches has been focused on linear molecular systems and single electronic state processes.

In this work, we will theoretically study the induced coherent electron currents and the ultrafast magnetic field generation of triatomic molecule H_3^{2+} by circularly polarized pulses. Due to the effect of the circularly polarized pulses, the coherent superposition of multiple electronic states gives rise to electron ring current in molecules. The electron dynamics of H_3^{2+} molecule is investigated by two channels: the coherent resonant excitation and the direct single-photon ionization. By investigating electron dynamics of H_3^{2+} molecule on its natural attosecond scale, we can realize the quantum control of the ultrafast magnetic field generation.

2. Theoretical method

In our simulation, we numerically solve the two-dimensional (2D) time-dependent Schrödinger equation (TDSE), which can exactly describe the excitation and ionization dynamics of H_3^{2+} molecule. As illustrated in Fig. 1(a), the H_3^{2+} molecule oriented in the (x, y) plane. The centroid coordinate system is used and the coordinate of the three protons

*Project supported by the National Natural Science Foundation of China (Grant Nos. 12074146 and 12074142).

†Corresponding author. E-mail: gjing@jlu.edu.cn

satisfied the centroid equation

$$x_i = \frac{\sum m_i x_i}{\sum m_i} = 0, \quad y_i = \frac{\sum m_i y_i}{\sum m_i} = 0.$$

The corresponding TDSE of H_3^{2+} molecule under Born–Oppenheimer approximation (BOA) can be expressed as follows:

$$\mathrm{i}\frac{\partial \Psi(\boldsymbol{r},t)}{\partial t} = [H_0(\boldsymbol{r}) + \boldsymbol{r}\cdot\boldsymbol{E}(t)]\,\Psi(\boldsymbol{r},t), \tag{1}$$

where

$$H_0(\boldsymbol{r}) = \frac{\boldsymbol{P}^2}{2} + V(\boldsymbol{r})$$

is the field-free Hamiltonian and $\boldsymbol{P}$ is the electron momentum. $V(\boldsymbol{r})$ is the soft-core Coulomb potential of the H_3^{2+} molecule. $\boldsymbol{r} \equiv (x,y)$ is in the two-dimensional x–y plane.

The molecular soft-core Coulomb potential can be written as

$$\begin{aligned} V(x,y) = & -\frac{1}{\sqrt{(x-0)^2 + (y-\frac{2}{3}R\cos\frac{\Theta}{2})^2 + c}} \\ & -\frac{1}{\sqrt{(x+R\sin\frac{\Theta}{2})^2 + (y+\frac{1}{3}R\cos\frac{\Theta}{2})^2 + c}} \\ & -\frac{1}{\sqrt{(x-R\sin\frac{\Theta}{2})^2 + (y+\frac{1}{3}R\cos\frac{\Theta}{2})^2 + c}}, \end{aligned} \tag{2}$$

where the soft parameter $c = 0.35$ is used to remove the singularity of Coulomb potential and obtain the precise energies of certain electronic state in H_3^{2+} molecule.[23] R is the distance between two protons and the bond angle $\Theta = 60^\circ$. For H_3^{2+} molecule, at internuclear distance $R = 4$ a.u., the three lowest electronic states are A′, E^+, and E^-. The excited electronic states $E^\pm$, are degenerate with E-symmetry and obtained as $\psi_{E^\pm} = (\psi_E^{(1)} \pm \mathrm{i}\psi_E^{(2)})/\sqrt{2}$,[23] corresponding to angular momentum $m \pm 1$ around the z axis. The two orthogonal real components $\psi_E^{(1)}$ and $\psi_E^{(2)}$ are obtained by solving TDSE with imaginary-time evolution method. In Fig. 1(b), we present the initial electron density of A′ electronic state obtained by solving TDSE with imaginary-time evolution method. One sees that the A′ electronic state can be approximated as a combination of 1s orbitals of three H atoms. Moreover, the corresponding molecular orbital obtained by the Gaussian09 program[24] are shown in Fig. 1(c), which is in good agreement with the initial electron density distributions obtained by the imaginary-time evolution method. The corresponding ionization potentials are respectively $I_p(A') = 1.08$ a.u. (29.38 eV) and $I_p(E^+) = I_p(E^-) = 0.923$ a.u. (25.02 eV).[23]

The circularly polarized laser pulse is used to investigate the electron dynamics in molecules.[20,23,25] The interaction between the electron and the laser pulse is $\boldsymbol{r}\cdot\boldsymbol{E}(t) = xE_x(t)\hat{e}_x + yE_y(t)\hat{e}_y$ under the length gauge and dipole approximation in the (x,y) plane. The expression of the circularly polarized laser pulse is as follows:

$$\boldsymbol{E}(t) = E_0 f(t)\,[\cos(\omega t)\hat{e}_x + \sin(\omega t)\hat{e}_y], \tag{3}$$

which propagates along the z axis with polarization direction $\hat{e}_x$ and $\hat{e}_y$ in the (x,y) plane. A $\sin^2(\pi t/nT_0)$ envelope $f(t)$ is adopted, where $T_0 = 2\pi/\omega$ is the optical cycle (o.c.). This pulse satisfies the total zero area $\int E(t)\mathrm{d}t = 0$.[26] The 2D TDSE in Eq. (1) is numerically solved by a second-order split-operator method combined with fast Fourier transform (FFT) technique.[27,28] The time step is fixed at $\Delta t = 0.01$ a.u. (1 a.u. = 24 as) and the spatial steps are $\Delta x = \Delta y = 0.25$ a.u. (1 a.u. = $1a_0$). The total spatial length is 128 a.u. The $\cos^{1/8}$ mask function is used to suppress unphysical effects generating from the reflection of the wave packet from the boundary. And the absorption boundary is set to $|x,y| = 40$ a.u.

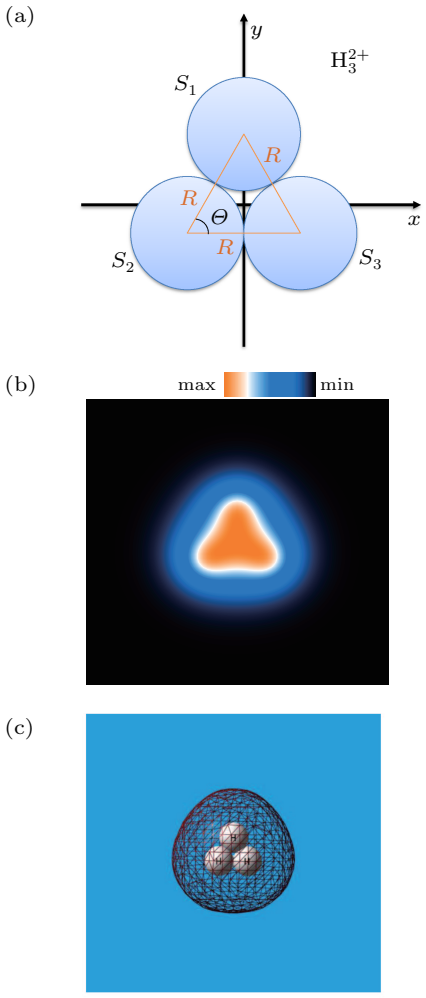

Fig. 1. (a) H_3^{2+} molecule oriented in the (x,y) plane. S_i (i = 1, 2, and 3) denotes the s orbital of the atomic H on proton i. R is the distance between two protons and the bond angle $\Theta = 60^\circ$. (b) The A′ electronic state of H_3^{2+} molecule calculated by imaginary-time evolution method. (c) Illustration of the A′ orbital of H_3^{2+} molecule obtained by Gaussian09.

The quantum expression of the time-dependent electronic

current density in the length gauge can be written as[29,30]

$$\boldsymbol{j}(\boldsymbol{r},t)=\frac{\mathrm{i}}{2}\left[\psi(\boldsymbol{r},t)\nabla_{\boldsymbol{r}}\psi^{*}(\boldsymbol{r},t)-\psi^{*}(\boldsymbol{r},t)\nabla_{\boldsymbol{r}}\psi(\boldsymbol{r},t)\right], \quad (4)$$

where

$$\nabla_{\boldsymbol{r}}=\frac{\partial}{\partial x}\boldsymbol{i}+\frac{\partial}{\partial y}\boldsymbol{j},$$

and $\psi(\boldsymbol{r},t)$ is the time-dependent electron wave packet obtained from Eq. (1). The corresponding time-dependent magnetic field $\boldsymbol{B}(\boldsymbol{r},t)$ is obtained by using the following classical Jefimenko's equation:[31]

$$\boldsymbol{B}(\boldsymbol{r},t)=\frac{\mu_0}{4\pi}\int\left[\frac{\boldsymbol{j}(\boldsymbol{r}',t_r)}{|\boldsymbol{r}-\boldsymbol{r}'|^3}+\frac{1}{|\boldsymbol{r}-\boldsymbol{r}'|^2c}\frac{\partial\boldsymbol{j}(\boldsymbol{r}',t_r)}{\partial t}\right]\times(\boldsymbol{r}-\boldsymbol{r}')\,\mathrm{d}^3\boldsymbol{r}', \quad (5)$$

where $t_r=t-r/c$ is the retarded time and $\mu_0=4\pi\times10^7$ NA^{-2} (6.692×10^{-4} a.u.). For the static-induced magnetic field after the laser pulse, equation (5) reduces to the classical Biot-Savart law.[31]

3. Results and discussion

The purpose of the present work is to investigate the induced electron current and generation of ultrafast magnetic field of H_3^{2+} molecule, with cyclic geometry, due to ultrafast negative charge migration in molecules. We investigate the electronic dynamics of H_3^{2+} molecule in two cases: (i) the coherent resonant excitation[20] and (ii) the direct single-photon ionization, which is shown in Fig. 2. For the coherent resonant excitation, the left-handed circularly polarized laser pulse leads to the charge migration from A′ state to E^+ state. The energy difference between A′ state and E^+ state is $E_{E^+}-E_{A'}\approx0.15$ a.u., which is corresponding to the laser wavelength $\lambda=300$ nm ($\omega=0.152$ a.u.). For the direct single-photon ionization, we adopt a laser field with the wavelength $\lambda=30$ nm ($\omega=1.52$ a.u.) leading to a direct single-photon ionization process since the photon energy $\omega>I_p$ ($I_p=1.08$ a.u.). The pulse intensity is $I_0=1.375\times10^{13}$ W·cm^{-2} ($E_0=0.0198$ a.u.) with duration of $10T_0$, where $T_0=2\pi/\omega$, (*i.e.*, 1 o.c. is 1000 as for 300 nm, 100 as for 30 nm) are fixed. The wave function propagates freely for $2T_0$ after the end of laser pulses.

In Figs. 3(a) and 3(b), we display the density distributions of the electron wave packet around the peak of pulse. From Fig. 3(a) one sees that the electron is localized and the coherent electron wave packet moves counterclockwise among the three protons periodically. The duration of one cycle is about $T_0=1000$ as, approximately equal to one cycle of the laser field with 300 nm. Besides, the electron density distribution presents symmetric structures on y axis at time $t=5.25$ o.c., 5.75 o.c., and asymmetric structures on y axis at time $t=5.0$ o.c., 5.5 o.c., 6.0 o.c. However, from Fig. 3(b) one sees that the electron density distribution maintains a symmetric structure, which do not depend on the time.

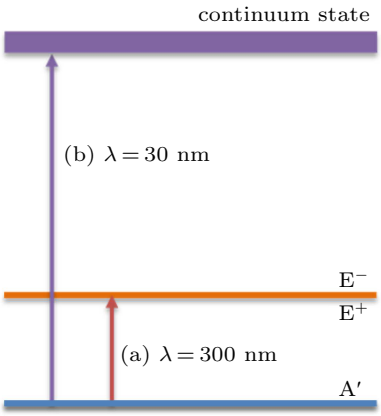

Fig. 2. Illustration of resonance excitation and direct ionization in our scheme: (a) the coherent resonant excitation arises between A′ state and E^+ state in H_3^{2+} molecule by $\lambda=300$ nm ($\omega=0.152$ a.u.) circularly polarized laser pulses; (b) the direct ionization from the A′ state to the continuum state after one-photon absorption by a circularly polarized laser pulse with wavelength $\lambda=30$ nm ($\omega=1.52$ a.u.).

The circularly polarized pulse with the wavelength of $\lambda=300$ nm, leads to the charge migration from A′ state to E^+ state. A coherent resonant excitation between the two electronic states arises after one-photon absorption which leads to a coherent superposition state. The resulting coherent superposition state wave function can be represented as[32]

$$\psi_0(\boldsymbol{r},t)=c_{A'}\psi_{A'}(\boldsymbol{r})\,\mathrm{e}^{-\mathrm{i}E_{A'}t}+c_{E^+}\psi_{E^+}(\boldsymbol{r})\,\mathrm{e}^{-\mathrm{i}E_{E^+}t}, \quad (6)$$

where $\psi_{A'/E^+}(\boldsymbol{r})$ and E_{A'/E^+} are the wave functions and energies of the A′ state or E^+ state, c_{A'/E^+} is the occupation coefficients.[20] The corresponding spatial distributions of coherent electron density as functions of time are described by

$$\begin{aligned}\mathcal{A}(\boldsymbol{r},t)&=|\psi_0(\boldsymbol{r},t)|^2\\&=\mathcal{A}^{(A')}(\boldsymbol{r})+\mathcal{A}^{(E^+)}(\boldsymbol{r})+\mathcal{A}^{(A',E^+)}(\boldsymbol{r},t),\end{aligned} \quad (7)$$

where $\mathcal{A}^{(A')}(\boldsymbol{r})=|c_{A'}\psi_{A'}(\boldsymbol{r})|^2$ and $\mathcal{A}^{(E^+)}(\boldsymbol{r})=|c_{E^+}\psi_{E^+}(\boldsymbol{r})|^2$, and $\mathcal{A}^{(A',E^+)}(\boldsymbol{r},t)$ is the interference term,

$$\mathcal{A}^{(A',E^+)}(\boldsymbol{r},t)\sim|c_{A'}(t)c_{E^+}(t)||\psi_{A'}(\boldsymbol{r})\psi_{E^+}(\boldsymbol{r})|\cos(\Delta Et), \quad (8)$$

where $\Delta E=E_{E^+}-E_{A'}$ is the energy difference between the A′ state and E^+ state. The interference term $\mathcal{A}^{(A',E^+)}(\boldsymbol{r},t)$ is time-dependent, which describes the attosecond coherent electronic migration.[33] The oscillation period of the interference term is $\nabla\tau^{(0)}=2\pi/\Delta E=T_0$. Thus, the time-dependent coherent electron density distributions depend on the interference term of the A′ state and E^+ state. At $\Delta Et=n\pi$, $t=nT_0/2$, where n is an integer, the interference term $\cos(\Delta Et)=\pm1$ leads to the maximum asymmetric structures of the electron density distributions, whereas at $\Delta Et=(n+1/2)\pi$, $t=(n+1/2)(T_0/2)$ and $\cos(\Delta Et)=0$, symmetric structures are produced, as shown in Fig. 3(a). For the direct single-photon ionization, the electron

is ionized from the A′ state to the continuum state by absorbing one-photon. Thus, the coherent superposition state does not exist anymore. As a result, the electron density distributions cannot be influenced by the coherent effects, so it present a symmetric structure, which do not depend on the time, as illustrated in Fig. 3(b).

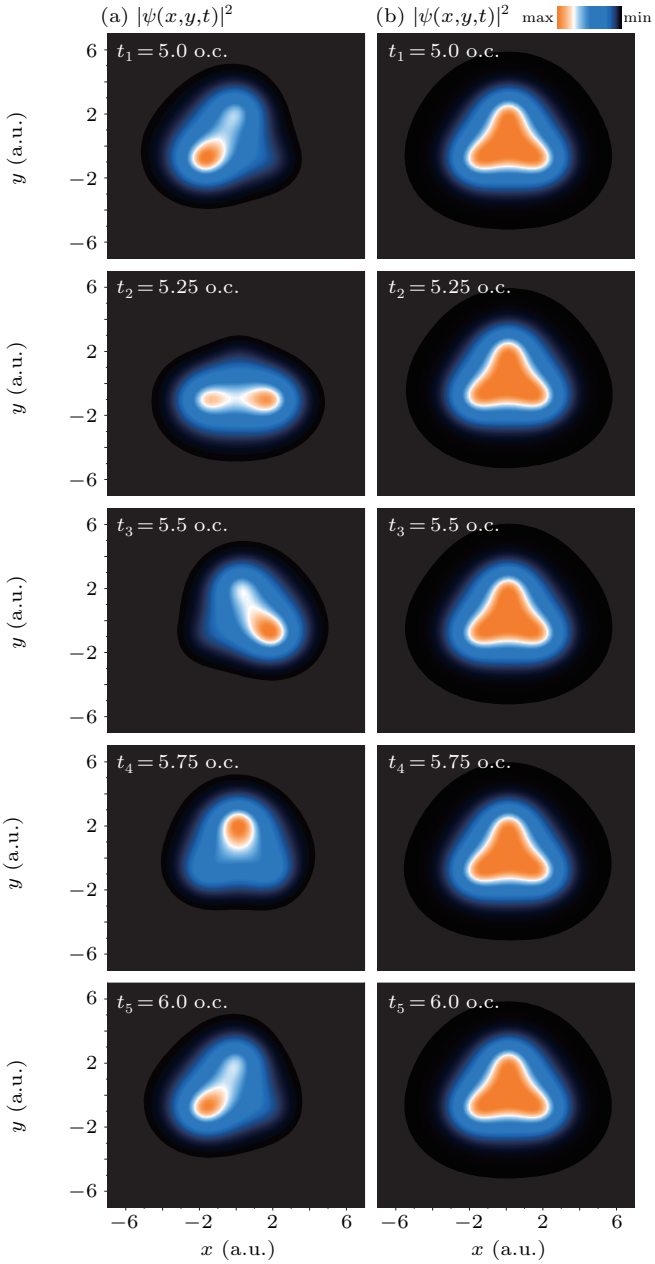

Fig. 3. Density distributions of the electron wave packet $p(x,y,t) = |\psi(x,y,t)|^2$ in the (x,y) plane at different moments ranging from $t = 5T_0$ to $6T_0$: (a) the coherent resonant excitation and (b) the direct single photon ionization.

Based on the evolution of the electron density distributions, we further investigate the induced electron ring current inside molecules. We show the distributions of the induced electronic current densities $\boldsymbol{j}(\boldsymbol{r},t)$ at various moments in Figs. 4(a)–4(b). The white arrows represent the directions of the electronic currents. In Fig. 4(a) for the coherent resonant excitation case, we see that the induced ring electronic current evolves counterclockwise with a period of $T_0 = 1000$ as. Besides, the evolution of the electronic current is approximately in phase with the rotation of the coherent electron wave packets. It is shown that the time-dependent electron current produced in charge migration attributed to the periodical evolution of the coherent electron wave packet between the protons. In Fig. 4(b) for the direct single-photon ionization case, we see that the ring current also evolves with a counterclockwise direction. The period is $T_0 = 100$ as. And the structure of electron current density is similar as that of the electron density distribution in Fig. 3(b).

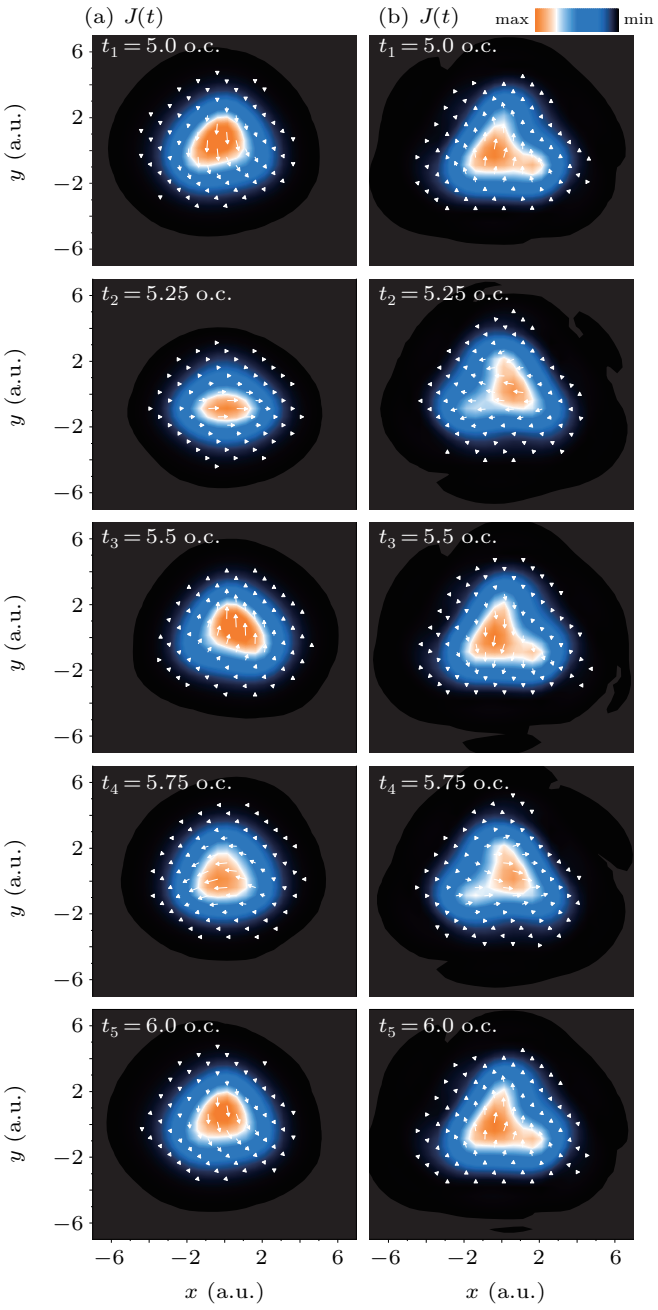

Fig. 4. The electronic current distributions for different times ranging from $t = 5T_0$ to $6T_0$. The white arrows label the directions of the electronic currents. (a) The coherent resonant excitation and (b) the direct single-photon ionization.

In order to better observe the variation of electron current

with time, we investigate the electronic currents by integrating $\boldsymbol{j}(\boldsymbol{r},t)$ over the section from $r=0$ to $r=\infty$. Since the electronic current is continuous, the probability of the electron currents being measured through any cross sections originated from the center point are equal.[21] The integral equation of Eq. (4) along the x axis can be written as[34]

$$\boldsymbol{J}(t)=\int_{-\infty}^{0}\boldsymbol{j}(x,0,t)\cdot\hat{e}_y\,\mathrm{d}x, \tag{9}$$

where $\boldsymbol{j}(\boldsymbol{r},t)=j_x(\boldsymbol{r},t)\hat{e}_x+j_y(\boldsymbol{r},t)\hat{e}_y$ and $\hat{e}_{x,y}$ are the unit vector along x and y directions. As shown in Figs. 5(a) and 5(b), the electronic currents $\boldsymbol{J}(t)$ oscillate periodically with time t resembling a cosine function and the oscillation period is about one optical cycle. Moreover, the change in intensity of the electronic currents with time is approximated in phase with the amplitude change of the driving pulse. It is shown that the intensity of the electronic currents is sensitive to the amplitude of the driving pulse. In Fig. 5(a) we can see that for the coherent resonant excitation case, the intensity of the induced electronic current reaches the maximum value 0.0195 a.u. at 5.0 o.c. Of note is that after the pulse being switched off ($t>10$ o.c.), the weak electronic current still exist and oscillates with a period $T=0.67T_0$. According to the coherence of electron wave packets, the coherent electron wave packets still spread spatially after the pulse being switched off and its quick spread results in a shorter oscillation period of induced electronic current, compared with the case of the pulse being switched on. In Fig. 4(b) for the direct single-photon ionization case, we find that the intensity of the induced electronic current also reaches its maximum value 0.0015 a.u. at 5.0 o.c. However, the electronic current will not exist after the pulse being switched off since there is no coherent electron wave packet.

In Figs. 5(a) and 5(b), we label the five moments t_1–t_5 which corresponds to the Figs. 4(a) and 4(b) with red crosses. From five moments in Fig. 5(a), one can see that the value of the electronic current is positive at $t_2=5.25$ o.c., $t_3=5.5$ o.c., whereas it is negative at $t_1=5.0$ o.c., $t_4=5.75$ o.c., $t_5=6.0$ o.c. At $t_2=5.25$ o.c. and $t_4=5.75$ o.c., the intensity is close to 0. From five moments in Fig. 5(b), one can see that the value of the electronic current is positive at $t_1=5.0$ o.c., $t_4=5.75$ o.c., $t_5=6.0$ o.c., while it is negative at $t_2=5.25$ o.c., $t_3=5.5$ o.c. Similar as that in Fig. 5(a), the intensity of the electronic current is also close to 0 at $t_2=5.25$ o.c. and $t_4=5.75$ o.c. The direction of electronic current are different in two cases at time $t\rightarrow t+T_0/2$ as illustrated in Figs. 4(a) and 4(b). The results show that the induced electronic currents oscillate periodically with different phases in two cases and the intensity of the coherent resonant excitation case is approximately one order of magnitude larger than that of direct ionization case. Since the electrons are ionized to the continuum state for the direct single-photon ionization case, the induced electronic current mainly comes from the free electrons in the continuum state, thus leading to a weak electronic current inside the molecules. And the oscillation of the electronic current is affected by coherent electron wave packet for case of the coherent resonant excitation.

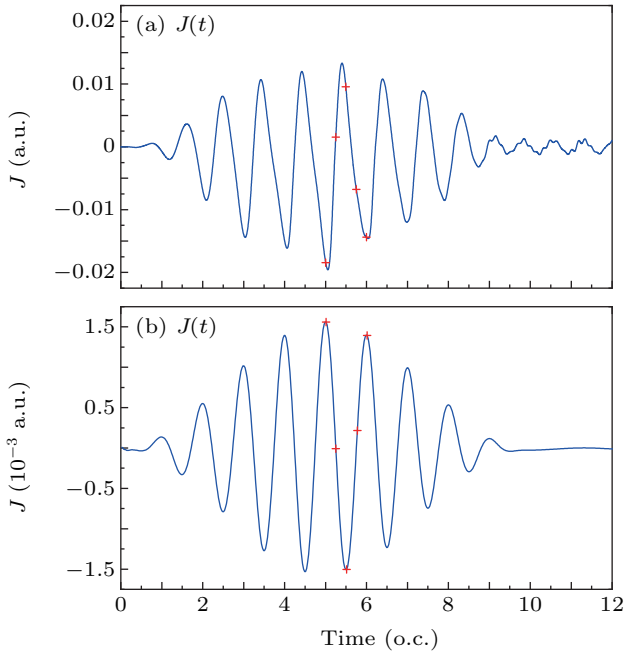

Fig. 5. Illustration of the time-dependent electronic currents for two cases (a) the coherent resonant excitation and (b) the direct single-photon ionization, the red crosses label five moments $t_1=5.0$ o.c., $t_2=5.25$ o.c., $t_3=5.5$ o.c., $t_4=5.75$ o.c., $t_5=6.0$ o.c. respectively.

The induced time-dependent electronic current can generate an internal ultrafast magnetic field in the molecule. In Figs. 6(a) and 6(b), we display the time-dependent magnetic fields $\boldsymbol{B}(\boldsymbol{r}=0,t)$ at the molecular center generated by the electronic currents $\boldsymbol{j}(\boldsymbol{r},t)$, which are shown in Figs. 5(a) and 5(b). According to classical physics,[35] the direction of generated magnetic fields mainly along the z axis, perpendicular to the (x,y) plane. The generated magnetic field also has dependence on the molecular orbitals. Figures 6(a) and 6(b) show the generation of magnetic fields with different intensities and phases at every nuclear centers. Due to the spiral effect of the circularly polarized laser pulse, the generated magnetic fields at every nuclear centers are not equivalent. The magnetic field $\boldsymbol{B}(\boldsymbol{r}=0,t)$ at the molecular center arises from the electron current, which is determined by the coherent superposition of the wavefunctions of the three protons. It is found that the time-dependent magnetic fields oscillate periodically with a period T_0, which indicate the electron coherence of the currents. As shown in Figs. 6(a) and 6(b), one can see that the oscillating magnetic field still exist after the pulse being switched off for the case of coherent resonant excitation, whereas the magnetic field does not exist anymore after the pulse being switched off for the case of direct single-photon ionization. The evolution of the magnetic field can be predicted by the induced electronic currents as illustrated in

Figs. 5(a) and 5(b), confirming the coherence of the electron. The results show that for the coherent resonant excitation the enhanced magnetic field $\boldsymbol{B}(\boldsymbol{r}=0,t)$ has the maximum value 0.27 T, whereas for the direct single-photon ionization case the maximum value is 0.015 T. The difference of the magnetic fields about two cases is associated with the electronic currents, and is also dependent on the photoionization process in molecules. Consequently, one can control the magnetic fields by adjusting the laser parameters. And the photoionization process encoded in the electron currents can be reconstructed with spatial and temporal resolutions by generated magnetic fields.

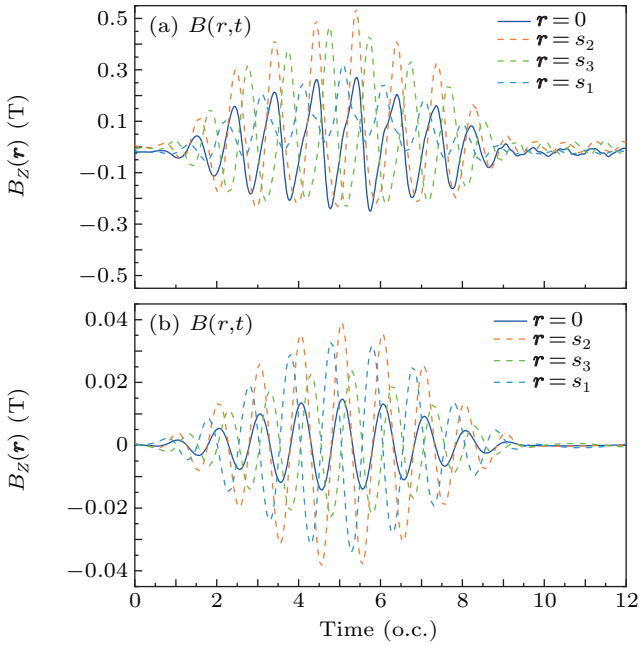

Fig. 6. Illustration of the time-dependent magnetic fields at the molecular center $\boldsymbol{r}=0$ and the three molecular proton centers, generated by the electronic currents corresponding to those in Figs. 5(a) and 5(b) for (a) the coherent resonant excitation and (b) the direct single-photon ionization.

4. Conclusion

We use the triatomic molecule with cyclic geometry H_3^{2+} as a benchmark system to investigate the induced electronic current and the generation of ultrafast magnetic field. Results from numerical solutions of the molecular TDSE show that the induced electronic currents and the generated magnetic fields depend on the photoionization process of molecules in intense laser fields. We calculated the electronic current and magnetic field in two cases: the coherent resonant excitation and the direct single-photon ionization. The circularly polarized pulses with wavelengths $\lambda = 300$ nm and $\lambda = 30$ nm are adopted respectively. For case of the coherent resonant excitation, with the asymmetric distributions of the coherent superposition as functions of t, the enhanced electron current arises subsequently, leading to the enhanced magnetic field generation. Moreover, the periodical evolution of the coherent electron wave packet leads to the fact that the electronic current oscillates periodically, which can produce oscillating magnetic fields. For the direct single-photon ionization, the electron is ionized from the A′ state to the continuum state by absorbing one-photon. So, the coherent superposition state does not exist anymore. Since the induced electronic current mainly comes from the free electrons in the continuum state, it can generate a relative weak magnetic field. The results show that both the electronic current and the magnetic field have different phases in the two cases. Moreover, the intensity of the coherent resonant excitation case is approximately one order of magnitude larger than that of direct ionization case. One can modulate the electronic current and the magnetic field by adjusting the parameters of the driving field. So, exploring the photoionization process in molecules is essential for controlling of the electronic current and the ultrafast magnetic field in molecule. In principle, our work can be used to explore the electronic dynamics in ring-molecules systems, presenting a general scheme which can also suitable for different atoms and molecules, and this scheme has great potential for ultrafast magnetism and electron dynamics.

References

[1] Chelkowski S, Corkum P B and Bandrauk A D 1999 *Phys. Rev. Lett.* **82** 3416
[2] Beylerian C and Cornaggia C 2004 *J. Phys. B* **37** L259
[3] Zuo T, Bandrauk A D and Corkum P B 1996 *Chem. Phys. Lett.* **259** 313
[4] Meckel M, Comtois D, Zeidler D, Staudte A, Bandulet H C, Kieffer J C, Villeneuve D M and Corkum P B 2008 *Science* **320** 1478
[5] Blaga C I, Xu J, DiChiara A D, Sistrunk E, Zhang K, Agostini P, Miller T A, DiMauro L F and Lin C D 2012 *Nature* **483** 194
[6] Liu X, Amini K, Steinle T, Sanchez A, Shaikh M, Belsa B, Steinmetzer J, Le A T, Moshammer R, Pfeifer T, Ullrich J, Moszynski R, Lin C D, Grfe S and Biegert J 2019 *J. Chem. Phys.* **151** 024306
[7] Gaumnitz T, Jain A, Pertot Y, Huppert M, Jordan I and Ardana-Lamas F 2017 *Opt. Express* **25** 27506
[8] Yuan K J and Bandrauk A D 2016 *J. Chem. Phys.* **145** 194304
[9] Huppert M, Jordan I, Baykusheva D and von Conta A 2016 *Phys. Rev. Lett.* **117** 093001
[10] Weinkauf R, Schanen P, Metsala A, Schlag E W, Brgle M and Kessler H 1996 *J. Phys. Chem.* **100** 18567
[11] Weinkauf R, Schlag E W, Martinez T J and Levine R D 1997 *J. Phys. Chem. A* **101** 7702
[12] Barth I and Manz J 2007 *Phys. Rev. A* **75** 012510
[13] Yuan K J and Bandrauk A D 2013 *Phys. Rev. A* **88** 013417
[14] Sederberg S, Kong F, Hufnagel F, Zhang C, Karimi E and Corkum P B 2020 *Nat. Photon.* **14** 680
[15] Lange K K, Tellgren E I, Hoffmann M R and Helgaker T 2012 *Science* **337** 327
[16] Matos-Abiague A and Berakdar J 2005 *Phys. Rev. Lett.* **94** 166801
[17] La-O-Vorakiat C, Turgut E, Teale C A, Kapteyn H C, Murnane M M, Mathias S, Aeschlimann M, Schneider C M, Shaw J M, Nembach H T and Silva T J 2012 *Phys. Rev. X* **2** 011005
[18] Bigot J Y, Vomir M and Beaurepaire E 2009 *Nat. Phys.* **5** 515
[19] Stanciu C D, Hansteen F, Kimel A V, Kirilyuk A, Tsukamoto A, Itoh A and Rasing T 2007 *Phys. Rev. Lett.* **99** 047601
[20] Yuan K J, Guo J and Bandrauk A D 2018 *Phys. Rev. A* **98** 043410
[21] Zhang X, Zhu X, Wang D, Li L, Liu X, Liao Q, Lan P and Lu P 2019 *Phys. Rev. A* **99** 013414
[22] Nobusada K and Yabana K 2007 *Phys. Rev. A* **75** 032518
[23] Yuan K J and Bandrauk A D 2020 *Phys. Chem. Chem. Phys.* **22** 325
[24] Frisch M, Trucks G, Schlegel H B, Scuseria G E, Robb M A, Cheeseman J R, Scalmani G, Barone V, Mennucci B, Petersson G, *et al.*, Inc., 2009 Inc., Wallingford CT **201**
[25] Yuan K J, Shu C C, Dong D and Bandrauk A D 2017 *J. Phys. Chem. Lett.* **8** 2229

[26] Krausz F and Ivanov M 2009 *Rev. Mod. Phys.* **81** 163

[27] Peters M, Nguyen-Dang T T, Cornaggia C, Saugout S, Charron E, Keller A and Atabek O 2011 *Phys. Rev. A* **83** 051403(R)

[28] Zhu X, Liu X, Li Y, Qin M, Zhang Q, Lan P and Lu P 2015 *Phys. Rev. A* **91** 043418

[29] Zhao K, Zhang Q, Chini M, Wu Y, Wang X and Chang Z 2012 *Opt. Lett.* **37** 3891

[30] Guo J, Yuan K J, Lu H and Bandrauk A D 2019 *Phys. Rev. A* **99** 053416

[31] Jefimenko O D 1989 *Electricity and Magnetism: An Introduction to the Theory of Electric and Magnetic Fields* (Electret Scientific Company)

[32] Bandrauk A D, Chelkowski S and Nguyen H S 2004 *Int. J. Quantum Chem.* **100** 834

[33] Kraus P M, Mignolet B, Baykusheva D, Rupenyan A and Bandrauk A D 2015 *Science* **350** 790

[34] Mineo H, Lin S H and Fujimura Y 2013 *J. Chem. Phys.* **138** 074304

[35] Halliday D, Resnick R and Walker J 2013 *Fundamentals of physics* (John Wiley and Sons)